View metadata, citation and similar papers at core.ac.uk

brought to you by CORE

provided by Digital Repository @ Iowa State University

IOWA STATE UNIVERSITY
Digital Repository

Physics and Astronomy Publications

Physics and Astronomy

9-1-2014

# Effects of isovalent substitution and pressure on the interplane resistivity of single-crystal Ba(Fe1-xRux)(2)As-2

Makariy A. Tanatar
*Iowa State University and Ames Laboratory*, tanatar@ameslab.gov

M. S. Torikachvili
*Iowa State University and San Diego State University*

A. Thaler
*Iowa State University and Ames Laboratory*

Sergey L. Bud'ko
*Iowa State University and Ames Laboratory*, budko@ameslab.gov

Paul C. Canfield
*Iowa State University and Ames Laboratory*, canfield@ameslab.gov

*See next page for additional authors*

Follow this and additional works at: https://lib.dr.iastate.edu/physastro_pubs

 Part of the Condensed Matter Physics Commons

The complete bibliographic information for this item can be found at https://lib.dr.iastate.edu/physastro_pubs/599. For information on how to cite this item, please visit http://lib.dr.iastate.edu/howtocite.html.

This Article is brought to you for free and open access by the Physics and Astronomy at Iowa State University Digital Repository. It has been accepted for inclusion in Physics and Astronomy Publications by an authorized administrator of Iowa State University Digital Repository. For more information, please contact digirep@iastate.edu.

# Effects of isovalent substitution and pressure on the interplane resistivity of single-crystal Ba(Fe1-xRux)(2)As-2


## Abstract

Temperature-dependent interplane resistivity ρc(T) was measured in an isovalent substituted iron-arsenide compound Ba(Fe1−xRux)2As2 over a substitution range from parent compound to slightly below optimal doping x=0.29. The feature of interest in the ρc(T), a broad resistivity crossover maximum found in the parent compound at Tmax≈200 K, shifts to higher temperatures with Ru substitution, ∼340 K for x=0.161 and goes out of the 400 K range for x=0.29. Nearly T-linear dependence of interplane resistivity is found at the highest substitution level x=0.29. This temperature-dependent ρc and its evolution with substitution bear close similarity to another type of isovalent substituted system BaFe2(As1−xPx)2. Similarly to the isovalent substitutions, the measurements of interplane resistivity in the parent BaFe2As2 compound under pressures up to 20 kbar also revealed a rapid rise in Tmax.



## Disciplines

Condensed Matter Physics

## Comments

This article is published as Tanatar, M. A., M. S. Torikachvili, A. Thaler, S. L. Bud'ko, P. C. Canfield, and R. Prozorov. "Effects of isovalent substitution and pressure on the interplane resistivity of single-crystal Ba (Fe 1− x Ru x) 2 As 2." *Physical Review B* 90, no. 10 (2014): 104518. DOI: 10.1103/PhysRevB.90.104518. Posted with permission.



## Authors

Makariy A. Tanatar, M. S. Torikachvili, A. Thaler, Sergey L. Bud'ko, Paul C. Canfield, and Ruslan Prozorov



This article is available at Iowa State University Digital Repository: https://lib.dr.iastate.edu/physastro_pubs/599

# Effects of isovalent substitution and pressure on the interplane resistivity of single-crystal $Ba(Fe_{1-x}Ru_x)_2As_2$

M. A. Tanatar,[1,2,*] M. S. Torikachvili,[2,3] A. Thaler,[1,2] S. L. Bud'ko,[1,2] P. C. Canfield,[1,2] and R. Prozorov[1,2]

[1]*Ames Laboratory, Ames, Iowa 50011, USA*

[2]*Department of Physics and Astronomy, Iowa State University, Ames, Iowa 50011, USA*

[3]*Department of Physics, San Diego State University, San Diego, California 92182, USA*

(Received 2 June 2014; revised manuscript received 11 August 2014; published 26 September 2014)

Temperature-dependent interplane resistivity $\rho_c(T)$ was measured in an isovalent substituted iron-arsenide compound $Ba(Fe_{1-x}Ru_x)_2As_2$ over a substitution range from parent compound to slightly below optimal doping $x = 0.29$. The feature of interest in the $\rho_c(T)$, a broad resistivity crossover maximum found in the parent compound at $T_{max} \approx 200$ K, shifts to higher temperatures with Ru substitution, ~340 K for $x = 0.161$ and goes out of the 400 K range for $x = 0.29$. Nearly $T$-linear dependence of interplane resistivity is found at the highest substitution level $x = 0.29$. This temperature-dependent $\rho_c$ and its evolution with substitution bear close similarity to another type of isovalent substituted system $BaFe_2(As_{1-x}P_x)_2$. Similarly to the isovalent substitutions, the measurements of interplane resistivity in the parent $BaFe_2As_2$ compound under pressures up to 20 kbar also revealed a rapid rise in $T_{max}$.

DOI: 10.1103/PhysRevB.90.104518 PACS number(s): 74.70.Xa, 72.15.−v, 74.25.Dw

## I. INTRODUCTION

A magnetically mediated mechanism of superconductivity in iron-based materials is discussed in relation to the observation of a quantum critical point in the phase diagram. In $BaFe_2As_2$ based superconductors, in which superconductivity can be induced by different types of substitutions and pressure, in all cases the maximum $T_c$ is not far from a point where magnetism vanishes as a function of the tuning parameter [1–5]. The existence of a quantum critical point governs systematic evolution of all electronic properties, in particular of the electrical resistivity.

The most clear evolution is found in the isovalent substituted material $BaFe_2(As_{1-x}P_x)_2$ [6]. Here resistivity for both in-plane $\rho_a$ and interplane $\rho_c$ current directions reveals extended range of $T$-linear dependence at optimal doping [6,7], and signatures of the quantum critical point are found in both normal and superconducting state properties [6,8,9]. Much more complex evolutions of in-plane and interplane resistivity are found in electron-doped $Ba(Fe_{1-x}Co_x)_2As_2$ [10–12] and hole-doped $Ba_{1-x}K_xFe_2As_2$ [13]. Here a dominant feature of $\rho_c(T)$ is a broad crossover maximum, which in the $BaFe_2As_2$ parent compound takes place at $T_{max} \approx 200$ K. This maximum shifts to lower temperatures with Co doping and does not change position with K doping up to $x = 0.34$ [13]. The maximum in $\rho_c(T)$ for the hole-doped materials correlates well with a slope-change feature in the in-plane transport [13,14].

We correlated the maximum in $\rho_c(T)$ with an anomaly in the temperature-dependent magnetic susceptibility [11], as found most clearly in the temperature-dependent NMR Knight shift measurements [15,16]. This interpretation suggests that the maximum is caused by the onset of activation of carriers over a minimum of the pseudogap, while the pseudogap maximum and restoration of normal metallic properties correspond to significantly higher temperatures and becomes visible only at very high electron dopings $x > 0.16$ [11]. The existence of pseudogap in iron-based superconductors was later confirmed with spectroscopic [17–19] and ARPES [20,21] techniques. Some recent advanced dynamical mean-field theory (DMFT) band structure calculations [22–24] also predict the existence of the pseudogap with strong orbital selectivity. The prediction is that the effect would be the strongest in the $d_{z^2}$ orbital [23], which would naturally lead to a much stronger effect in the interplane transport.

This interpretation of the resistivity maximum is not unique though. The characteristic energy scale $T_{max}$ is significantly smaller than the energies found in band structure calculations [22–24]. An alternative interpretation is the loss of spin-disorder scattering at low temperatures, though this effect alone cannot explain resistivity decrease with temperature above $T_{max}$. Clearly additional studies are required to get a new insight into an anomalous resistivity behavior at high temperatures. It is of particular interest if the unique evolution of resistivity observed in the phosphorus-doped materials can be found in other systems. Isovalent substitution of Fe by Ru in $BaFe_2As_2$ also suppresses magnetism and brings about superconductivity. Importantly Ru substitution does not lead to changes of the Fermi surface beyond the suppression of the folding effects of the magnetic wave vector [25]. Ru substitution was also shown to act similar to application of pressure [26–28]. Study of the interplane resistivity using pressure as a tuning parameter provides an additional possibility to tune the system without introducing substitution disorder, inevitable for all types of dopings and particularly strong when substitutions are made in the Fe site. With this motivation in mind here we perform a systematic study of the interplane transport in $BaFe_2As_2$ compound using isovalent Ru substitution and pressure as tuning parameters. We find that the evolution of the resistivity in samples with Ru substitution is similar with that observed on isovalent substitution of As with P. A broad range of $T$-linear dependence is observed in both in-plane and interplane transport in samples with close to optimal substitution level. The general trend of shifting the maximum in $\rho_c(T)$ for parent $BaFe_2As_2$ to higher

*Corresponding author: tanatar@ameslab.gov

 ©2014 American Physical Society

temperatures with pressure is similar to the effects of two isovalent substitutions, P for As and Ru for Fe. However, using the temperature of the structural/magnetic transition as a reference, the rate at which $T_{max}$ increases is notably higher for pressure than for the isoelectron substitutions.

## II. EXPERIMENT

Single crystals of $Ba(Fe_{1-x}Ru_x)_2As_2$ (BaRu122) were grown using a high temperature FeAs flux technique [26]. The samples from the same batches have some distribution of $T_c$. As a first step of sample selection for our study, we cleaved thin slabs typically of 20 $\mu$m thickness with two clean cleavage surfaces from the inner part of the crystals. Numerous smaller pieces with sides along (100) directions for resistivity measurements were further cleaved using a razor blade. The samples for interplane resistivity measurements typically had dimensions of $0.5 \times 0.5 \times 0.02\,mm^3$ size ($a \times b \times c$). Elongated samples for in-plane resistivity measurements typically were of $1 \times 0.2 \times 0.02\,mm^3$ size. All samples were prescreened using magneto-optical imaging [29–31] and the dipper version of the tunnel diode resonator (TDR) technique [32,33]. These measurements allowed us to exclude samples with macroscopic inhomogeneity and possible inclusions with lower $T_c$.

Both in-plane and interplane resistivity were measured on big sets of crystals coming from the same slab. Conventional four-probe measurements were performed on samples with ultralow contact resistance (typically 10 $\mu\Omega$) soldered contacts [31,34]. For interplane resistivity measurements we relied on negligible contact resistance and used a two-probe technique. Top and bottom surfaces of the samples were covered with Sn solder and 50 $\mu$m diameter silver wires were attached to enable measurements in a four-probe configuration, which was used down to the sample to measure series connected sample $R_s$ and contact $R_c$ resistance. Taking into account that typical sample resistance $R_s$ is 1 m$\Omega$, and contact resistance $R_c \sim 10\,\mu\Omega$, the contact resistance represents a minor correction of the order of 1% to 5%. The validity of the assumption $R_s \gg R_c$ can be directly seen for our samples for temperatures below the superconducting $T_c$, where $R_s = 0$ and the measured resistance represents $R_c$ [10,29,31]. The details of the measurement procedure can be found in Refs. [10,11,35]. Measurements on samples with $c \ll a$ are very sensitive to any inhomogeneity in the contact resistance or internal sample connectivity, which tend to mix the in-plane component $\rho_a$ due to redistribution of the current. Measurements on a large number of samples are necessary in order to select the ones with minimal intraplane meandering. Typically this screening process involved at least five samples from each batch yielding the same dipper TDR $T_c$. In all cases we obtained qualitatively similar temperature dependencies of the electrical resistivity. The resistivity value at room temperature $\rho_c$(300 K) was approximately in the range 1000 to 1500 $\mu\Omega$ cm. The resistivity value for in-plane resistivity $\rho_a$(300 K) was in the $300 \pm 50$ $\mu\Omega$ cm range and did not reveal any evolution with $x$ beyond error bars, contrary to previous reports suggesting significant decrease [36,37].

The measurements of electrical resistivity under pressure were carried out with a piston-cylinder Be-Cu pressure cell, with a core of tungsten carbide. The sample, manganin, and Pb manometers were mounted on a feedthrough, which was inserted into a Teflon capsule filled with a 60:40 mixture of *n*-pentane: light mineral oil, which served as the pressure transmitting medium. Pressure was generated at ambient temperature with a hydraulic press, using manganin as a reference manometer. The pressure was locked in, and the cell was then loaded into a Quantum Design Physical Property Measurement System (PPMS-9), which provided the temperature environment for the measurements, as well as the dc measurements of resistance for the sample, manometers, and a Cernox temperature sensor attached to the body of the cell. The pressure at low temperatures was determined from the superconducting transition temperature of the Pb manometer. The cooling and warming rates were kept below 0.35 K/min, which maintained the $T$ lag between the Cernox sensor and the sample well bellow 0.5 K throughout the whole temperature range. In light of the approximately linear variation of pressure from ambient temperature to ~90 K in piston-cylinder cells [38], the pressure values at temperatures between these limits were estimated from linear interpolation.

## III. RESULTS

### A. Interplane resistivity in samples with isovalent Ru substitution

Figure 1 shows the evolution of the in-plane (top panel) and interplane resistivity (bottom panel) of samples of isovalent substituted $Ba(Fe_{1-x}Ru_x)_2As_2$. The in-plane resistivity data are very similar to previous reports on the same material [26,36,37]. The main feature of $\rho_a(T)$ is a gradual drop of the temperature of coinciding structural/magnetic transition $T_{sm}$ [26,39,40], which goes away at $x \approx 0.29$. For all $x \leqslant 0.24$ we still see the presence of slight $\rho_a(T)$ up-turn on cooling above $T_c$, which is completely suppressed for $x = 0.29$. The data for sample $x = 0.29$ reveal very close to $T$-liner dependence over a broad range from above $T_c$ to almost 400 K, with only a mild slope change at around 200 K. The temperature of the slope change in $\rho_a(T)$ is reminiscent of the much more pronounced feature in the $\rho_a(T)$ of hole-doped materials $(Ba_{1-x}K_x)Fe_2As_2$ [13,14,41]. A previous study on a higher doped materials [37] suggested that eventually, at $x \approx 0.35$, $\rho_a(T)$ becomes $T$ linear over the whole temperature range from $T_c$ to 300 K.

Evolution of the interplane transport in isovalent substituted $Ba(Fe_{1-x}Ru_x)_2As_2$ is distinctly different from both electron-doped BaCo122 [11] and hole-doped BaK122 [13] materials. The interplane resistivity $\rho_c(T)$ reveals a broad crossover maximum at $T_{max}$, which, with Ru substitution, moves from approximately 200 to above 300 K in samples with $x = 0.21$. The $\rho_c(T)$ data for $x \geqslant 0.24$ suggest that the substitution drives $T_{max}$ past 400 K, the highest temperature of our measurements. However, the leftover of the maximum can be found in a mild slope change in samples with $x = 0.24$ and $x = 0.29$, marked with squares in the bottom panel of Fig. 1. This evolution trend suggests that in samples with higher substitution level both in-plane and interplane resistivity would become $T$ linear, similar to BaP122 materials.

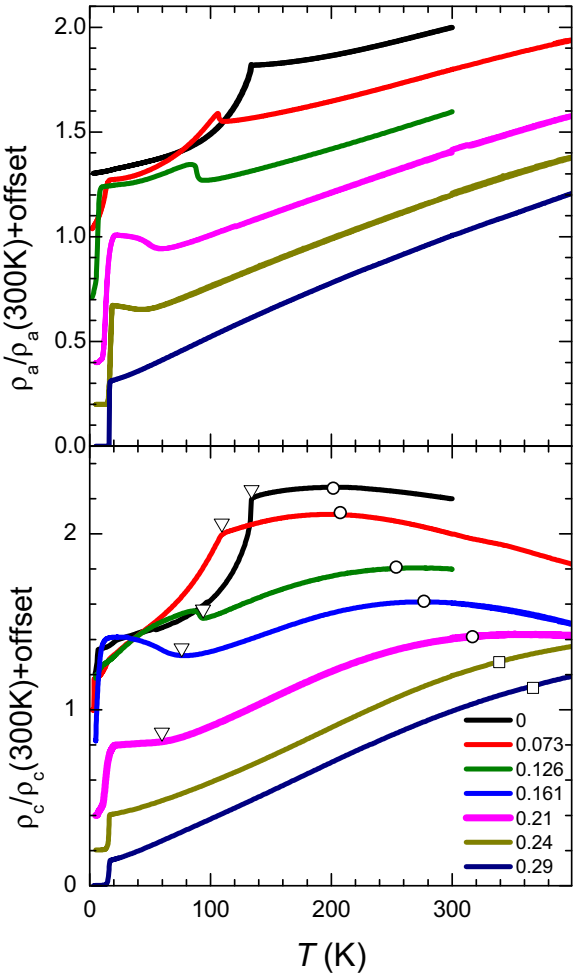


FIG. 1. (Color online) Top panel: Doping evolution of the temperature-dependent in-plane resistivity of $Ba(Fe_{1-x}Ru_x)_2As_2$. The curves are presented using normalized $\rho/\rho(300\ K)$ plots and offset for clarity. Top to bottom $x = 0$, 0.073, 0.126, 0.21, 0.24, and 0.29. Bottom panel: Temperature-dependent interplane resistivity of $Ba(Fe_{1-x}Ru_x)_2As_2$, top to bottom $x = 0$, 0.073, 0.126, 0.161, 0.21, 0.24, and 0.29. Down triangles show positions of the coupled structural/magnetic transition, open circles show positions of $T_{max}$. For the highest substitutions $x = 0.24$ and 0.29 no maximum is observed in the range, but a slope change crossover is still clearly visible, as indicated by the square symbols.

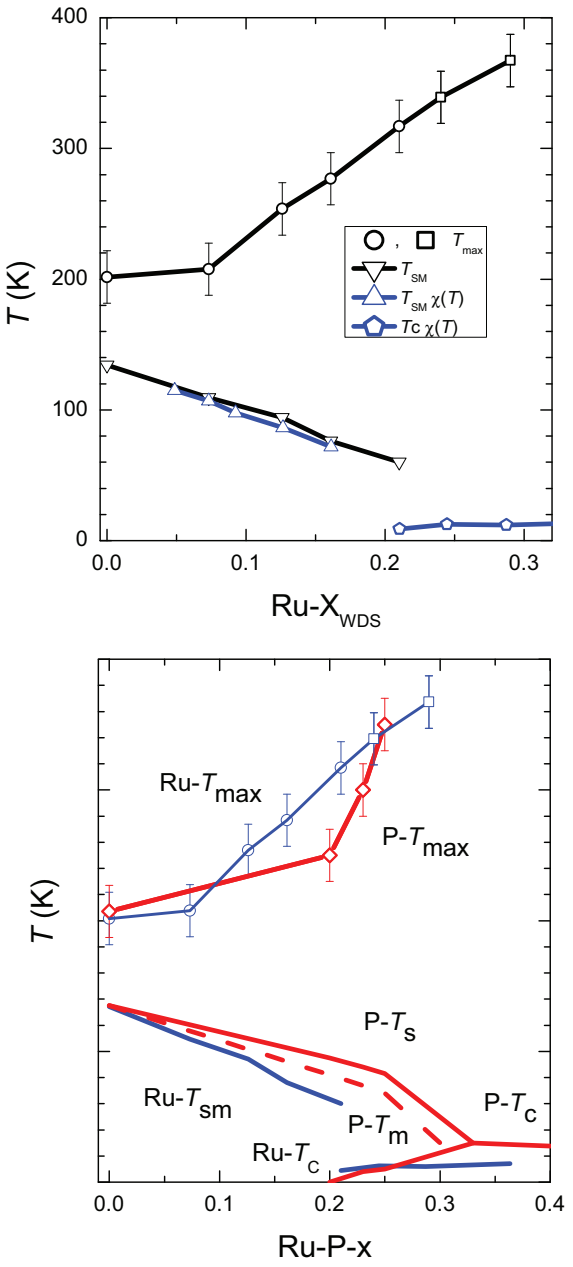


FIG. 2. (Color online) Top panel shows the compositional phase diagram of $Ba(Fe_{1-x}Ru_x)_2As_2$ as determined from interplane resistivity measurements in this study (down triangles, circles, and open squares, see Fig. 1 for definition) in comparison with magnetization measurements (up triangles and pentagons) of Thaler *et al.* [26]. Bottom panel compares temperature-composition diagrams for two isovalent substitutions, of Fe with Ru (blue lines and symbols) and of As with P (red lines and symbols) [6,7].

The top panel of Fig. 2 summarizes the evolution of the main features of the temperature-dependent interplane resistivity with Ru substitution. For reference we show the temperatures of the coupled magnetic/structural transition and bulk superconducting $T_c$ as determined from magnetization measurements [26]. The temperature of the interplane resistivity maximum $T_{max}$ moves up very rapidly with $x$, similar to the behavior in isovalent substituted $BaFe_2(As_{1-x}P_x)_2$. In the bottom panel we directly compare the phase diagrams of the two isovalent substitutions in $BaFe_2As_2$, which indeed reveal clear similarity. Keeping in mind the uncertainties in compositional determination $x$, the potential effect of disorder on the phase diagram [42], and the uncertainty in the determination of the maximum position due to possible admixture of the $\rho_a(T)$ component, the similarity of the two phase diagrams is just remarkable.

### B. Comparison of different types of substitutions

To put our findings in a broader perspective, in Fig. 3 we directly compare the temperature-dependent interplane resistivity of $BaFe_2As2$ derived compositions with four different

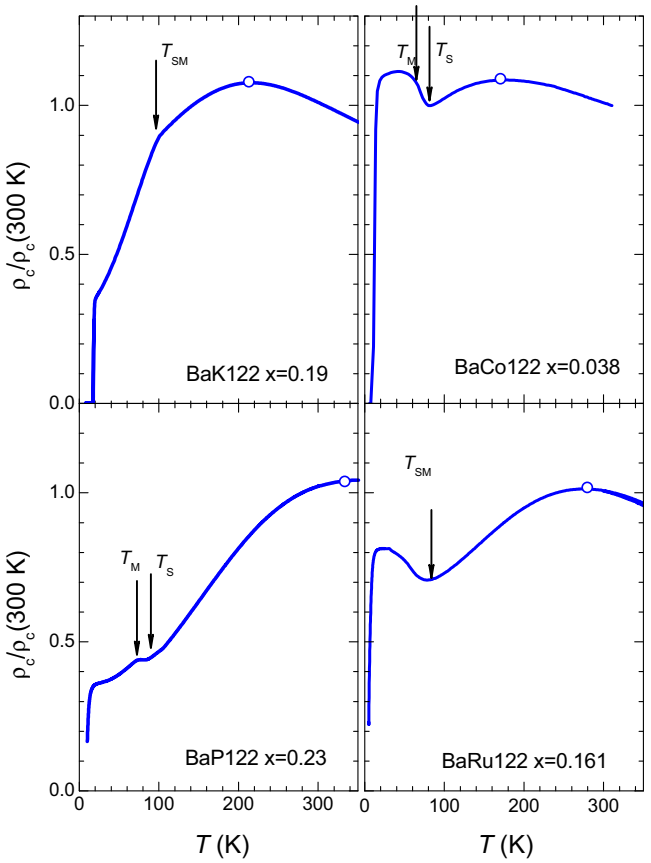


FIG. 3. (Color online) Comparison of the temperature-dependent interplane resistivity of underdoped samples of $BaFe_2As_2$ based superconductors, for the compositions selected to have comparable $T_{sm}$ of about 100 K. Top left panel (a) shows $\rho_c(T)$ for hole-doped $(Ba_{1-x}K_x)Fe_2As_2$ [13], top right panel (b) for electron-doped $Ba(Fe_{1-x}Co_x)_2As_2$ [11], bottom left panel (c) for isovalent substituted $BaFe_2(As_{1-x}P_x)_2$ [7], and bottom right panel (d) for isovalent substituted $Ba(Fe_{1-x}Ru_x)_2As_2$ (this study). Note the very different evolution of the position of maximum of interplane resistivity $T_{max}$, shown with open circles.

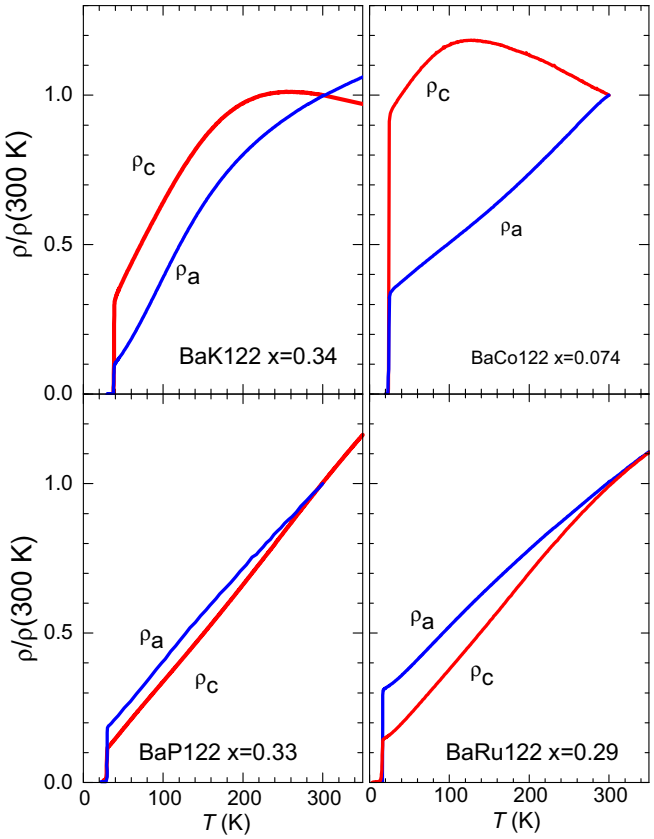


FIG. 4. (Color online) Comparison of the temperature-dependent in-plane (blue lines) and interplane (red lines) resistivity of close to optimally doped samples of $BaFe_2As_2$ based superconductors. Top left panel (a) shows data for hole-doped $(Ba_{1-x}K_x)Fe_2As_2$ [13], top right panel (b) for electron-doped $Ba(Fe_{1-x}Co_x)_2As_2$ [11], bottom left panel (c) for isovalent substituted $BaFe_2(As_{1-x}P_x)_2$ [6,7], and bottom right panel (d) for isovalent substituted $Ba(Fe_{1-x}Ru_x)_2As_2$ (this study). Note that Ru-doped samples are actually underdoped, which is the most likely reason that the evolution towards $T$-linear dependence is incomplete.

types of substitutions in the "underdoped" regime. For the sake of comparison we selected compositions with similar $T_{sm} \sim 100$ K. This selection criterion in fact does not correlate well with the superconductivity; samples with $T_{sm}$ in this range have significantly different $T_c$, and reveal just traces of superconductivity in BaP122 and BaRu122. Nevertheless, this comparison reveals interesting features. Samples with substitutions into the Fe site, Co and Ru, have significantly higher normalized residual resistivity $\rho(0)/\rho(300\,\mathrm{K}) = 1.1$ and 0.8, respectively, as compared to approximately 0.3 in BaP122 and BaK122. The values of $\rho_c(300\ \mathrm{K})$ in all cases are the same within error bars and are in the range 1000 to 1500 $\mu\Omega$ cm, so that the difference is in fact observed between actual resistivity values. This finding is a natural consequence of the substitution disorder introduced right into orbitals forming the states at the Fermi energy. Second, there is a robust upturn in $\rho_c(T)$ just below $T_{sm}$ in samples with more disorder, while the increase is not as pronounced in samples with substitution away from the Fe site.

In Fig. 4 we compare temperature-dependent in-plane (blue lines) and interplane (red lines) resistivity of samples of $BaFe_2As_2$ derived superconductors with four different types of substitutions at close to optimal level. As suggested by the $T$-$x$ phase diagrams, Fig. 2, two different types of isovalent substitutions yield quite similar temperature-dependent resistivity, as indicated in the two bottom panels in Fig. 4. Neither $\rho_a(T)$ nor $\rho_c(T)$ in BaP122 and BaRu122 show any evident slope-change features for optimal substitution level, which is in stark contrast with hole-doped BaK122 revealing maximum in $\rho_c(T)$ and slope change in $\rho_a(T)$ at around 200 K [13,14], and with electron-doped BaCo122 [11,12], showing crossover only in the interplane transport.

### C. Evolution of the temperature-dependent interplane resistivity with pressure

It is remarkable that two different types of isovalent substitution give rise to similar effects on both the in-plane and interplane temperature-dependent electrical resistivity. It was shown previously that the effects of pressure and of

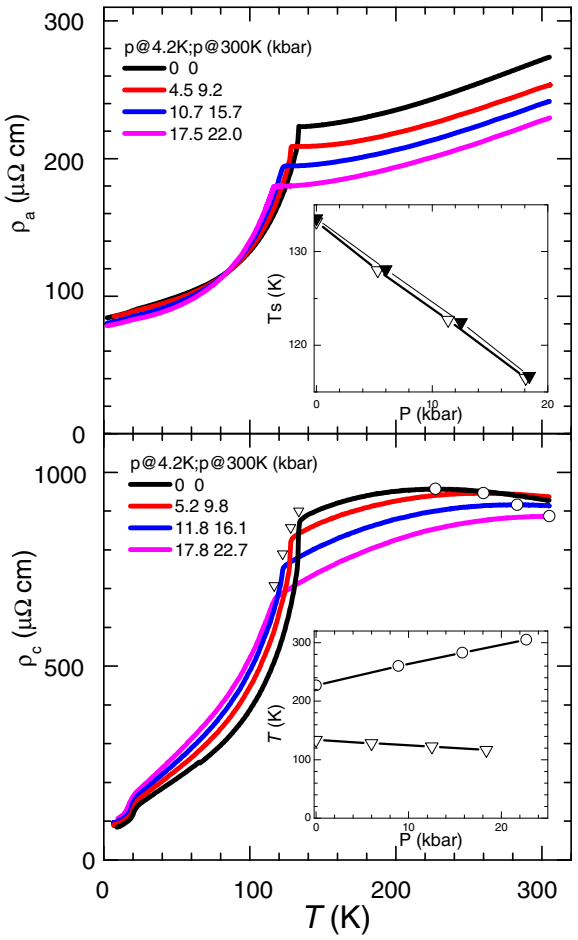


FIG. 5. (Color online) Evolution of the temperature-dependent in-plane (top panel) and interplane (bottom panel) resistivity with pressure in the parent compound of 122 iron-based superconductors $BaFe_2As_2$. Pressure values are changing on cooling, as shown for temperatures of 300 and 4.2 K. The inset in the top panel shows pressure dependence of $T_s$ as determined from $\rho_a$ (solid down triangles) and from $\rho_c$ (open down triangles) measurements. Inset in the bottom panel shows evolution of $T_s$ (down triangles) and of $T_{max}$ (circles) with pressure. Symbols in the main panel show the respective temperatures vs actual temperature-dependent resistivity curves.

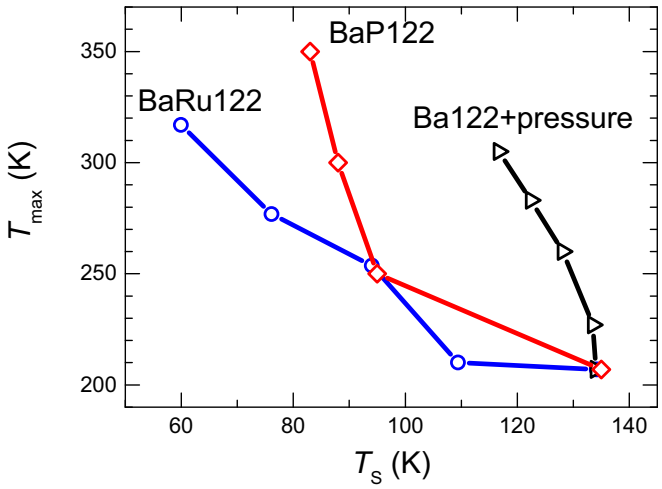


FIG. 6. (Color online) Evolution of the position of the maximum of the temperature-dependent interplane resistivity $T_{max}$ as a function of the structural transition temperature $T_S$ for cases of isovalent Ru (blue circles) and P (red diamonds) substitutions and of application of pressure (black right triangles). Note the significantly faster increase of $T_{max}$ under pressure.

the isovalent Ru substitution on in-plane resistivity are very similar [27,28]. In a way, pressure provides an independent tuning parameter for quantum criticality, which has a significant advantage: it does not introduce substitutional disorder. At the simplest approximation, pressure tunes the system by changing lattice parameters which in turn tune the bandwidth, so its effect can be significantly different from doping. Here we study evolution of the in-plane and interplane resistivity of parent $BaFe_2As_2$ with pressure.

In Fig. 5 we show evolution of in-plane (top panel) and interplane (bottom panel) resistivity of parent $BaFe_2As_2$ with pressure. Use of the piston-cylinder cell allowed us to reach pressures of about 20 kbar (at 4.2 K), which is not nearly sufficient to suppress magnetism of the parent compound [43], but acceptable to suppress $T_{sm}$ to close to 100 K, as was the case for samples shown in Fig. 3. As can be seen from inset in top panel of Fig. 5, the structural/magnetic transition shifts from 134 to about 115 K at the maximum pressure of our experiment. A very similar shift of $T_{sm}$ is observed from $\rho_c(T)$ measurements, shown for comparison in the inset with solid symbols. This comparison suggests that the $c$-axis resistivity measurements performed on samples with Sn soldered contacts covering the whole sample surface and which are strong enough to prevent samples from detwinning [44], do not significantly affect resistivity studies as a function of pressure.

Despite the limited pressure range, the maximum in the interplane resistivity at $T_{max}$ shows a quite significant shift to higher temperatures. It moves up from $T_{max} \sim 200$ K to almost 300 K in the pressure range studied. In Fig. 6 we compare the behavior of $T_{max}$ and $T_{sm}$ for parent Ba122 under pressure with their evolution upon Ru and P isovalent substitutions. As $T_{sm} \rightarrow 0$ as the system approaches a putative quantum critical point, this dependence reveals evolution of the features on its approach. Note that for BaP122 the structural and magnetic transitions are split with doping, while they remain coincident on Ru substitution [39,40]. As can be seen from Fig. 6, pressure is moving the maximum much faster than isovalent substitution.

The residual resistivity of $BaFe_2As_2$ does not change much with pressure, see Fig. 5. This reflects the fact that pressure does not change the degree of disorder in the samples. Simultaneously, this feature suggests that the electronic structure in the antiferromagnetic phase below $T_{sm}$ does not change with pressure. Application of pressure reduces both in-plane and interplane resistivity in the metallic phase above $T_{sm}$, suggestive of weakening electronic correlations. The inter-plane resistivity in the antiferromagnetic phase below $T_{sm}$, for example at 100 K [Fig. 5(b)], shows an increase, indicating an increase of spin scattering below the transition, consistent with increase of spin disorder with pressure. The overall pressure evolution of the

temperature-dependent resistivity is suggesting that the $T$-linear dependence of interplane resistivity can be eventually found at higher pressures corresponding to pressure-tuned QCP. Additional studies at higher pressures will be necessary in order to test this trend experimentally.

## IV. DISCUSSION

The pseudogap or partial gap on the Fermi surface [45] in the cuprates is well established by a number of spectroscopic techniques [46,47], however, its microscopic origin is still debated [48]. Main theories and experiments link it to either two neighboring phases, an antiferromagnetic Mott insulator, with pseudogap arising due to exotic magnetism [49], and superconductivity, as an effect of the preformed superconducting pairs [50], or to a competing charge order phase [51]. The pseudogap is universally observed in both hole- and electron-doped cuprates [52], though it is much more pronounced in the former.

Our previous study of electron-doped BaCo122 found a clear correlation between the maximum in the interplane resistivity and anomalies in the temperature-dependent Knight shift and spin relaxation time [11,16]. This correlation between the pseudogap features in resistivity and NMR measurements is also known in the cuprates [45]. Further similarity between the two families is strong asymmetry of the pseudogap features on electron- and hole-doped sides [45,52]. There are, however, some significant differences. In the cuprates the pseudogap vanishes close to optimum doping [47], while in electron-doped iron-based materials the superconducting dome is completely imbedded into the pseudogap range [11,15].

Because of the correlation between features in magnetic and resistive measurements, it is natural to consider magnetic origin of the pseudogap. Long-range magnetic order, developing in the parent $BaFe_2As_2$ below $T_m$, leads to two effects. Reconstruction of the Fermi surface [53,54] opens a gap on part of the Fermi surface, which is expected to give rise to resistivity increase. Simultaneously long-range magnetic ordering is accompanied by a loss of inelastic spin disorder scattering [55,56], which leads to an increase of the mean-free path, giving rise to resistivity decrease. The increase of the mean-free path is limited at low temperatures by elastic scattering on residual impurities. In the parent compound the loss of the spin-disorder scattering dominates and the resistivity decreases gradually below $T_m$, particularly strongly in the cleanest annealed samples [57]. The partial gapping is responsible for an increase of the resistivity below $T_m$ in Ru- and Co-substituted materials, see Fig. 3, in which contribution of spin-disorder scattering is small compared to impurity scattering, as evidenced by high residual resistivity value. The increase is mild in BaP122 and is virtually absent in BaK122 with significantly smaller residual resistivity.

Study of the in-plane resistivity anisotropy in strain-detwinned samples [44,58,59] found that actually resistivity increase starts at a structural transition at a temperature $T_s$ which is always higher than $T_m$ [60]. Based on this observation, it was suggested that the tetragonal-to-orthorhombic transition is also of magnetic origin and reflects directional nematic correlations between spins, without static long-range magnetic order [61–64]. These correlations lead to dramatically different effects for two directions in the plane, with resistivity increase for one direction of the current and the decrease for another [44,65]. Interestingly, strained samples reveal in-plane resistivity anisotropy at temperatures even significantly higher than $T_s$, showing that magnetic correlations (and thus nematic susceptibility) start significantly higher than actual long-range ordering below $T_m$ [66–68].

Following the same line of argument, it is natural to assign pseudogap features in the interplane resistivity to a build-up of magnetic correlations, reflected in NMR measurements [15,16,69]. Significant difference, though, is that the directional interplane transport would be most sensitive to the interplane magnetic correlations, which should be quite strong in proximity to three-dimensional magnetism, as found in $BaFe_2As_2$. Our observations of the different doping dependence of the pseudogap features for three types of substitutions may be suggestive that evolution of magnetic correlations proceeds significantly different in these cases. This difference may be also responsible for a difference between doping evolution of the pseudogap features in magnetically two-dimensional cuprates and magnetically three-dimensional iron-based materials.

## V. CONCLUSIONS

Isovalent Ru substitution in $Ba(Fe_{1-x}Ru_x)_2As_2$ leads to a systematic evolution of the temperature-dependent interplane resistivity towards a $T$-linear dependence at the optimal doping, in line with expectations for the scenario invoking existence of the quantum critical point in the substitutional phase diagram. The dominant high-temperature feature of the temperature-dependent interplane resistivity, a maximum at a temperature $T_{max}$, shifts rapidly to higher temperatures with $x$, revealing a trend similar to another type of isovalent substitution in $BaFe_2(As_{1-x}P_x)_2$ [7]. Because the two substitution series show different evolution of the Fermi surface [25,70], this similarity suggests that the maximum is not related to evolution of the electronic structure.

Our observations suggest that despite very different evolution of $T_{max}$ feature for four different types of dopings into parent $BaFe_2As_2$, there exists a similarity within each doping type irrespective of the chemical nature of substitution, a trend revealed in our previous studies of transition-metal substitutions in $Ba(Fe_{1-x}T_x)_2As_2$, $T$ = Co, Ni, Rh, Pd [11,12]. The faster rise of $T_{max}$ with application of hydrostatic pressure is suggestive that electronic bandwidth/correlations play important role in the appearance of the maximum.

## ACKNOWLEDGMENTS

This work was supported by the U.S. Department of Energy (DOE), Office of Science, Basic Energy Sciences, Materials Science and Engineering Division. The research was performed at the Ames Laboratory, which is operated for the U.S. DOE by Iowa State University under contract DE-AC02-07CH11358. M.S.T. gratefully acknowledges support from the National Science Foundation under Grant No. DMR-0805335.

[1] J. Paglione and R. L. Greene, Nat. Phys. **6**, 645 (2010).
[2] D. C. Johnston, Adv. Phys. **59**, 803 (2010).
[3] P. C. Canfield and S. L. Bud'ko, Annu. Rev. Condens. Matter Phys. **1**, 27 (2010).
[4] G. R. Stewart, Rev. Mod. Phys. **83**, 1589 (2011).
[5] L. Taillefer, Annu. Rev. Condens. Matter Phys. **1**, 51 (2010).
[6] S. Kasahara, T. Shibauchi, K. Hashimoto, K. Ikada, S. Tonegawa, R. Okazaki, H. Shishido, H. Ikeda, H. Takeya, K. Hirata, T. Terashima, and Y. Matsuda, Phys. Rev. B **81**, 184519 (2010).
[7] M. A. Tanatar, K. Hashimoto, S. Kasahara, T. Shibauchi, Y. Matsuda, and R. Prozorov, Phys. Rev. B **87**, 104506 (2013).
[8] Y. Nakai, T. Iye, S. Kitagawa, K. Ishida, H. Ikeda, S. Kasahara, H. Shishido, T. Shibauchi, Y. Matsuda, and T. Terashima, Phys. Rev. Lett. **105**, 107003 (2010)
[9] K. Hashimoto, K. Cho, T. Shibauchi, S. Kasahara, Y. Mizukami, R. Katsumata, Y. Tsuruhara, T. Terashima, H. Ikeda, M. A. Tanatar, H. Kitano, N. Salovich, R. W. Giannetta, P. Walmsley, A. Carrington, R. Prozorov, and Y. Matsuda, Science **336**, 1554 (2012).
[10] M. A. Tanatar, N. Ni, C. Martin, R. T. Gordon, H. Kim, V. G. Kogan, G. D. Samolyuk, S. L. Bud'ko, P. C. Canfield, and R. Prozorov, Phys. Rev. B **79**, 094507 (2009).
[11] M. A. Tanatar, N. Ni, A. Thaler, S. L. Bud'ko, P. C. Canfield, and R. Prozorov, Phys. Rev. B **82**, 134528 (2010).
[12] M. A. Tanatar, N. Ni, A. Thaler, S. L. Bud'ko, P. C. Canfield, and R. Prozorov, Phys. Rev. B **84**, 014519 (2011).
[13] M. A. Tanatar, W. E. Straszheim, H. Kim, J. Murphy, N. Spyrison, E. C. Blomberg, K. Cho, J.-Ph. Reid, B. Shen, L. Taillefer, H.-H. Wen, and R. Prozorov, Phys. Rev. B **89**, 144514 (2014).
[14] Y. Liu, M. A. Tanatar, W. E. Straszheim, B. Jensen, K. W. Dennis, R. W. McCallum, V. G. Kogan, R. Prozorov, and T. A. Lograsso, Phys. Rev. B **89**, 134504 (2014).
[15] F. L. Ning, K. Ahilan, T. Imai, A. S. Sefat, R. Jin, M. A. McGuire, B. C. Sales, and D. Mandrus, J. Phys. Soc. Jpn. **77**, 103705 (2008).
[16] F. L. Ning, K. Ahilan, T. Imai, A. S. Sefat, M. A. McGuire, B. C. Sales, D. Mandrus, P. Cheng, B. Shen, and H.-H. Wen, Phys. Rev. Lett. **104**, 037001 (2010).
[17] S. J. Moon, A. A. Schafgans, S. Kasahara, T. Shibauchi, T. Terashima, Y. Matsuda, M. A. Tanatar, R. Prozorov, A. Thaler, P. C. Canfield, A. S. Sefat, D. Mandrus, and D. N. Basov, Phys. Rev. Lett. **109**, 027006 (2012).
[18] S. J. Moon, A. A. Schafgans, M. A. Tanatar, R. Prozorov, A. Thaler, P. C. Canfield, A. S. Sefat, D. Mandrus, and D. N. Basov, Phys. Rev. Lett. **110**, 097003 (2013).
[19] S. J. Moon, Y. S. Lee, A. A. Schafgans, A. V. Chubukov, S. Kasahara, T. Shibauchi, T. Terashima, Y. Matsuda, M. A. Tanatar, R. Prozorov, A. Thaler, P. C. Canfield, S. L. Bud'ko, A. S. Sefat, D. Mandrus, K. Segawa, Y. Ando, and D. N. Basov, Phys. Rev. B **90**, 014503 (2014).
[20] Y.-M. Xu, P. Richard, K. Nakayama, T. Kawahara, Y. Sekiba, T. Qian, M. Neupane, S. Souma, T. Sato, T. Takahashi, H.-Q. Luo, H.-H. Wen, G.-F. Chen, N.-L. Wang, Z. Wang, Z. Fang, X. Dai, and H. Ding, Nat. Commun. **2**, 392 (2011).
[21] T. Shimojima *et al.*, Phys. Rev. B **89**, 045101 (2014).
[22] Z. P. Yin, K. Haule, and G. Kotliar, Nat. Mater. **10**, 932 (2011).
[23] M. Aichhorn, S. Biermann, T. Miyake, A. Georges, and M. Imada, Phys. Rev. B **82**, 064504 (2010).
[24] Ph. Werner, M. Casula, T. Miyake, F. Aryasetiawan, A. J. Millis, and S. Biermann, Nat. Phys. **8**, 331 (2012).
[25] R. S. Dhaka, C. Liu, R. M. Fernandes, R. Jiang, C. P. Strehlow, T. Kondo, A. Thaler, J. Schmalian, S. L. Bud'ko, P. C. Canfield, and A. Kaminski, Phys. Rev. Lett. **107**, 267002 (2011).
[26] A. Thaler, N. Ni, A. Kracher, J. Q. Yan, S. L. Bud'ko, and P. C. Canfield, Phys. Rev. B **82**, 014534 (2010).
[27] S. K. Kim, M. S. Torikachvili, E. Colombier, A. Thaler, S. L. Bud'ko, and P. C. Canfield, Phys. Rev. B **84**, 134525 (2011).
[28] S. K. Kim, Ph.D. thesis, Iowa State University, 2013.
[29] R. Prozorov, N. Ni, M. A. Tanatar, V. G. Kogan, R. T. Gordon, C. Martin, E. C. Blomberg, P. Prommapan, J. Q. Yan, S. L. Bud'ko, and P. C. Canfield, Phys. Rev. B **78**, 224506 (2008).
[30] R. Prozorov, M. A. Tanatar, B. Roy, N. Ni, S. L. Bud'ko, P. C. Canfield, J. Hua, U. Welp, and W. K. Kwok, Phys. Rev. B **81**, 094509 (2010).
[31] M. A. Tanatar, N. Ni, S. L. Bud'ko, P. C. Canfield, and R. Prozorov, Supercond. Sci. Technol. **23**, 054002 (2010).
[32] M. A. Tanatar, N. Spyrison, K. Cho, E. C. Blomberg, G. Tan, P. Dai, C. Zhang, and R. Prozorov, Phys. Rev. B **85**, 014510 (2012).
[33] N. Spyrison, M. A. Tanatar, K. Cho, Y. Song, P. Dai, C. Zhang, and R. Prozorov, Phys. Rev. B **86**, 144528 (2012).
[34] M. A. Tanatar, R. Prozorov, N. Ni, S. L. Bud'ko, and P. C. Canfield, U.S. Patent No. 8,450,246 (1 September 2011).
[35] M. A. Tanatar, N. Ni, G. D. Samolyuk, S. L. Bud'ko, P. C. Canfield, and R. Prozorov, Phys. Rev. B **79**, 134528 (2009).
[36] F. Rullier-Albenque, D. Colson, A. Forget, P. Thuéry, and S. Poissonnet, Phys. Rev. B **81**, 224503 (2010).
[37] M. J. Eom, S. W. Na, C. Hoch, R. K. Kremer, and J. S. Kim, Phys. Rev. B **85**, 024536 (2012).
[38] J. D. Thompson, Rev. Sci. Instrum. **55**, 231 (1984).
[39] M. G. Kim, D. K. Pratt, G. E. Rustan, W. Tian, J. L. Zarestky, A. Thaler, S. L. Bud'ko, P. C. Canfield, R. J. McQueeney, A. Kreyssig, and A. I. Goldman, Phys. Rev. B **83**, 054514 (2011).
[40] M. G. Kim, J. Soh, J. Lang, M. P. M. Dean, A. Thaler, S. L. Bud'ko, P. C. Canfield, E. Bourret-Courchesne, A. Kreyssig, A. I. Goldman, and R. J. Birgeneau, Phys. Rev. B **88**, 014424 (2013).
[41] B. Shen, H. Yang, Z.-S. Wang, F. Han, B. Zeng, L. Shan, C. Ren, and H.-H. Wen, Phys. Rev. B **84**, 184512 (2011).
[42] K. Cho, M. Kończykowski, J. Murphy, H. Kim, M. A. Tanatar, W. E. Straszheim, B. Shen, H. H. Wen, and R. Prozorov, Phys. Rev. B **90**, 104514 (2014).
[43] E. Colombier, S. L. Bud'ko, N. Ni, and P. C. Canfield, Phys. Rev. B **79**, 224518 (2009).
[44] M. A. Tanatar, E. C. Blomberg, A. Kreyssig, M. G. Kim, N. Ni, A. Thaler, S. L. Bud'ko, P. C. Canfield, A. I. Goldman, I. I. Mazin, and R. Prozorov, Phys. Rev. B **81**, 184508 (2010).
[45] T. Timusk and B. Statt, Rep. Prog. Phys. **62**, 61 (1999).
[46] T. Kondo, R. Khasanov, T. Takeuchi, J. Schmalian, and A. Kaminski, Nature (London) **457**, 296 (2009).
[47] I. M. Vishik, W. S. Lee, R.-H. He, M. Hashimoto, Z. Hussain, T. P. Devereaux, and Z.-X. Shen, New J. Phys. **12**, 105008 (2010).
[48] M. R. Norman, D. Pines, and C. Kallin, Adv. Phys. **54**, 715 (2005).
[49] V. Hinkov, P. Bourges, S. Pailhes, Y. Sidis, A. Ivanov, C. D. Frost, T. G. Perring, C. T. Lin, D. P. Chen, and B. Keimer, Nat. Phys. **3**, 780 (2007).

[50] K. K. Gomes, A. N. Pasupathy, A. Pushp, S. Ono, Y. Ando, and A. Yazdani, Nature (London) **447**, 569 (2007).
[51] See, for example, M. Vojta, Adv. Phys. **58**, 699 (2009).
[52] N. P. Armitage, P. Fournier, and R. L. Greene, Rev. Mod. Phys. **82**, 2421 (2010).
[53] J. G. Analytis, R. D. McDonald, J.-H. Chu, S. C. Riggs, A. F. Bangura, C. Kucharczyk, M. Johannes, and I. R. Fisher, Phys. Rev. B **80**, 064507 (2009).
[54] T. Terashima, N. Kurita, M. Tomita, K. Kihou, C.-H. Lee, Y. Tomioka, T. Ito, A. Iyo, H. Eisaki, T. Liang, M. Nakajima, S.i Ishida, S.-i. Uchida, H. Harima, and S. Uji, Phys. Rev. Lett. **107**, 176402 (2011).
[55] I. I. Mazin and M. D. Johannes, Nat. Phys. **5**, 141 (2009).
[56] E. C. Blomberg, M. A. Tanatar, R. M. Fernandes, I. I. Mazin, B. Shen, H.-H. Wen, M. D. Johannes, J. Schmalian, and R. Prozorov, Nat. Commun. **4**, 1914 (2013).
[57] S. Ishida, M. Nakajima, T. Liang, K. Kihou, C. H. Lee, A. Iyo, H. Eisaki, T. Kakeshita, Y. Tomioka, T. Ito, and S. Uchida, Phys. Rev. Lett. **110**, 207001 (2013).
[58] J.-H. Chu, J. G. Analytis, K. De Greve, P. L. McMahon, Z. Islam, Y. Yamamoto, and I. R. Fisher, Science **329**, 824 (2010).
[59] I. R. Fisher, L. Degiorgi, and Z. X. Shen, Rep. Progr. Phys. **74**, 124506 (2010).
[60] R. M. Fernandes, A. V. Chubukov, J. Knolle, I. Eremin, and J. Schmalian, Phys. Rev. B **85**, 024534 (2012).
[61] C. Xu, M. Muller, and S. Sachdev, Phys. Rev. B **78**, 020501(R) (2008), superconductors.
[62] C. Fang, H. Yao, W.-F. Tsai, J. P. Hu, and S. A. Kivelson, Phys. Rev. B **77**, 224509 (2008).
[63] B. Valenzuela, E. Bascones, and M. J. Calderón, Phys. Rev. Lett. **105**, 207202 (2010).
[64] R. M. Fernandes, A. V. Chubukov, and J. Schmalian, Nat. Phys. **10**, 97 (2014).
[65] E. C. Blomberg, M. A. Tanatar, A. Kreyssig, N. Ni, A. Thaler, Rongwei Hu, S. L. Bud'ko, P. C. Canfield, A. I. Goldman, and R. Prozorov, Phys. Rev. B **83**, 134505 (2011).
[66] E. C. Blomberg, A. Kreyssig, M. A. Tanatar, R. M. Fernandes, M. G. Kim, A. Thaler, J. Schmalian, S. L. Bud'ko, P. C. Canfield, A. I. Goldman, and R. Prozorov, Phys. Rev. B **85**, 144509 (2012).
[67] Y.-X. Yang, Y. Gallais, R. M. Fernandes, I. Paul, L. Chauvire, M.-A. Méasson, M. Cazayous, A. Sacuto, D. Colson, and A. Forget, JPS Conf. Proc. **3**, 015001 (2014).
[68] J.-H. Chu, H.-H. Kuo, J. G. Analytis, and I. R. Fisher, Science **337**, 710 (2012).
[69] S.-H. Baek, H.-J. Grafe, L. Harnagea, S. Singh, S. Wurmehl, and B. Büchner, Phys. Rev. B **84**, 094510 (2011).
[70] A. Carrington, Rep. Prog. Phys. **74**, 124508 (2011).